

This article appeared in a journal published by Elsevier. The attached copy is furnished to the author for internal non-commercial research and education use, including for instruction at the authors institution and sharing with colleagues.

Other uses, including reproduction and distribution, or selling or licensing copies, or posting to personal, institutional or third party websites are prohibited.

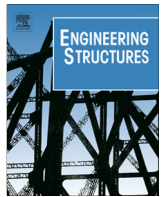
In most cases authors are permitted to post their version of the article (e.g. in Word or Tex form) to their personal website or institutional repository. Authors requiring further information regarding Elsevier's archiving and manuscript policies are encouraged to visit:

<http://www.elsevier.com/authorsrights>



Contents lists available at ScienceDirect

## Engineering Structures

journal homepage: [www.elsevier.com/locate/engstruct](http://www.elsevier.com/locate/engstruct)

## A simple and robust elastoplastic constitutive model for concrete

F. Poltronieri<sup>a</sup>, A. Piccolroaz<sup>a</sup>, D. Bigoni<sup>a,\*</sup>, S. Romero Baivier<sup>b</sup><sup>a</sup> Department of Civil, Environmental and Mechanical Engineering, University of Trento, Via Mesiano 77, I-38123 Trento, Italy<sup>b</sup> Vesuvius Group S.A., Rue de Douvrain 17, 7011 Ghlin, Belgium

## ARTICLE INFO

## Article history:

Received 12 March 2013

Revised 3 December 2013

Accepted 9 December 2013

Available online 11 January 2014

## Keywords:

Rock-like materials

Ceramics

Elastoplasticity

Hardening laws

## ABSTRACT

An elasto-plastic model for concrete, based on a recently-proposed yield surface and simple hardening laws, is formulated, implemented, numerically tested and validated against available test results. The yield surface is smooth and particularly suited to represent the behaviour of rock-like materials, such as concrete, mortar, ceramic and rock. A new class of isotropic hardening laws is proposed, which can be given both an incremental and the corresponding finite form. These laws describe a smooth transition from linear elastic to plastic behaviour, incorporating linear and nonlinear hardening, and may approach the perfectly plastic limit in the latter case. The reliability of the model is demonstrated by its capability of correctly describing the results yielded by a number of well documented triaxial tests on concrete subjected to various confinement levels. Thanks to its simplicity, the model turns out to be very robust and well suited to be used in complex design situations, as those involving dynamic loads.

© 2013 Elsevier Ltd. All rights reserved.

## 1. Introduction

The mechanical behaviour of concrete is rather complex – even under monotonic and quasi-static loading – because of a number of factors: (i) highly *nonlinear* and (ii) strongly *inelastic* response, (iii) *anisotropic* and (iv) eventually *localized* damage accumulation with (v) *stiffness degradation*, (vi) *contractive* and subsequently *dilatant* volumetric strain, leading to (vii) *progressively severe cracking*. This complexity is the macroscale counterpart of several concurrent and cooperative or antagonist micromechanisms of damage and stiffening, as for instance, pore collapse, microfracture opening and extension or closure, aggregate debonding, and interfacial friction. It can therefore be understood that the constitutive modelling of concrete (but also of similar materials such as rock, soil and ceramic) has been the subject of an impressive research effort, which, broadly speaking, falls within the realm of elastoplasticity,<sup>1</sup> where the term ‘plastic’ is meant to include the damage as a specific inelastic mechanism. In fact, elastoplasticity is a theoretical framework allowing the possibility of a phenomenological description of all the above-mentioned constitutive features of concrete in terms of: (i) yield function features, (ii) coupling elastic and plastic

deformation, (iii) flow-rule nonassociativity, and (iv) hardening sources and rules [3]. However, the usual problem arising from a refined constitutive description in terms of elastoplasticity is the complexity of the resulting model, which may lead to several numerical difficulties related to the possible presence of yield surface corners, discontinuity of hardening, lack of self-adjointness due to nonassociativity and failure of ellipticity of the rate equations due to strain softening. As a consequence, refined models often lack numerical robustness or slow down the numerical integration to a level that the model becomes of awkward, if not impossible, use. A ‘minimal’ and robust constitutive model, not obsessively accurate but able to capture the essential phenomena related to the progressive damage occurring during monotonic loading of concrete, is a necessity to treat complex load situations.

The essential ‘ingredients’ of a constitutive model are a convex, smooth yield surface capable of an excellent interpolation of data and a hardening law describing a smooth transition between elasticity and a perfectly plastic behaviour. Exclusion of strain softening, together with flow rule associativity, is the key to preserve ellipticity, and thus well-posedness of the problem. In the present paper, an elastoplastic model is formulated, based on the so-called ‘BP yield surface’ [3,4,11] which is shown to correctly describe the damage envelope of concrete, and on an infinite class of isotropic hardening rules (given both in incremental form and in the corresponding finite forms), depending on a hardening parameter. Within a certain interval for this parameter hardening is unbounded (with linear hardening obtained as a limiting case), while outside this range a smooth hardening/perfectly-plastic transition is described. The proposed model does not describe certain phenomena which are known to occur in concrete, such as for instance

\* Corresponding author. Tel.: +39 0461282507; fax: +39 0461282599.

E-mail address: [bigoni@ing.unitn.it](mailto:bigoni@ing.unitn.it) (D. Bigoni).URL: <http://www.ing.unitn.it/bigoni/> (D. Bigoni).

<sup>1</sup> The research on elastoplastic modelling of concrete has reached its apex in the seventies and eighties of the past century, when so many models have been proposed that are now hard to even only be summarized (see among others, [2,5,8,15]). Although nowadays other approaches are preferred, like those based on particle mechanics [13], the aim of the present article is to formulate a relatively simple and robust model, something that is difficult to be achieved with advanced models.

anisotropy of damage, softening, and elastic degradation, but provides a simple and robust tool, which is shown to correctly represent triaxial test results at high confining pressure.

## 2. Elastoplasticity and the constitutive model

This section provides the elastoplastic constitutive model in terms of incremental equations. The form of the yield surface is given, depending on the stress invariants and a set of material parameters. A new class of hardening laws is formulated in order to describe a smooth transition from linear elastic to plastic behaviour.

### 2.1. Incremental constitutive equations

The decomposition of the strain into the elastic ( $\epsilon_e$ ) and plastic ( $\epsilon_p$ ) parts as

$$\epsilon = \epsilon_e + \epsilon_p \quad (1)$$

yields the incremental elastic strain in the form

$$\dot{\epsilon}_e = \dot{\epsilon} - \dot{\epsilon}_p. \quad (2)$$

The 'accumulated plastic strain' is defined as follows:

$$\pi_a = \int_0^t |\dot{\epsilon}_p| d\tau, \quad (3)$$

where  $t$  is the time-like variable governing the loading increments. Introducing the flow rule

$$\dot{\epsilon}_p = \dot{\lambda} \mathbf{P}, \quad (4)$$

where  $\mathbf{P}$  is the gradient of the plastic potential, we obtain that the rate of the accumulated plastic strain is proportional to the plastic multiplier ( $\dot{\lambda} \geq 0$ ) as

$$\dot{\pi}_a = \dot{\lambda} |\mathbf{P}|. \quad (5)$$

A substitution of Eqs. (2) and (4) into the incremental elastic constitutive equation relating the increment of stress  $\dot{\sigma}$  to the increment of elastic strain  $\dot{\epsilon}_e$  through a fourth-order elastic tensor  $\mathbb{E}$  as  $\dot{\sigma} = \mathbb{E} \dot{\epsilon}_e$ , yields

$$\dot{\sigma} = \mathbb{E} \dot{\epsilon} - \dot{\lambda} \mathbb{E} \mathbf{P}. \quad (6)$$

Note that, for simplicity, reference is made to isotropic elasticity, so that the elastic tensor  $\mathbb{E}$  is defined in terms of elastic modulus  $E$  and Poisson's ratio  $\nu$ .

During plastic loading, the stress point must satisfy the yield condition  $F(\sigma, \mathbf{k}) = 0$  at every time increment, so that the Prager consistency can be written as

$$\dot{F} = \mathbf{Q} \cdot \dot{\sigma} + \frac{\partial F}{\partial \mathbf{k}} \cdot \dot{\mathbf{k}} = 0, \quad (7)$$

where  $\mathbf{Q} = \partial F / \partial \sigma$  is the yield function gradient and  $\mathbf{k}$  is the hardening parameters vector.

By defining the hardening modulus  $H(\sigma, \mathbf{k})$  as

$$\frac{\partial F}{\partial \mathbf{k}} \cdot \dot{\mathbf{k}} = -\dot{\lambda} H(\sigma, \mathbf{k}), \quad (8)$$

Eq. (7) can be rewritten in the form

$$\mathbf{Q} \cdot \dot{\sigma} - \dot{\lambda} H = 0 \quad (9)$$

Further, the plastic multiplier can be obtained from Eqs. (6) and (9)

$$\dot{\lambda} = \frac{\mathbf{Q} \cdot \mathbb{E} \dot{\epsilon}}{H + \mathbf{Q} \cdot \mathbb{E} \mathbf{P}}. \quad (10)$$

Finally, a substitution of Eqs. (10) into (6) yields the elasto-plastic constitutive equations in the rate form

$$\dot{\sigma} = \mathbb{E} \dot{\epsilon} - \frac{\mathbf{Q} \cdot \mathbb{E} \dot{\epsilon}}{H + \mathbf{Q} \cdot \mathbb{E} \mathbf{P}} \mathbb{E} \mathbf{P}, \quad (11)$$

where, for simplicity, the associative flow rule  $\mathbf{P} = \mathbf{Q}$ , will be adopted in the sequel.

### 2.2. The BP yield surface

The following stress invariants are used in the definition of the BP yield function [4]

$$p = -\frac{\text{tr} \sigma}{3}, \quad q = \sqrt{3} J_2, \quad \theta = \frac{1}{3} \cos^{-1} \left( \frac{3\sqrt{3}}{2} \frac{J_3}{J_2^{3/2}} \right), \quad (12)$$

where  $\theta \in [0, \pi/3]$  is the Lode's angle and

$$J_2 = \frac{1}{2} \text{tr} \mathbf{S}^2, \quad J_3 = \frac{1}{3} \text{tr} \mathbf{S}^3, \quad \mathbf{S} = \sigma - \frac{\text{tr} \sigma}{3} \mathbf{I}, \quad (13)$$

in which  $\mathbf{S}$  is the deviatoric stress and  $\mathbf{I}$  is the identity tensor.

The seven-parameters BP yield function  $F$  [4] is defined as

$$F(\sigma) = f(p) + \frac{q}{g(\theta)}, \quad (14)$$

in which the pressure-sensitivity is described through the 'meridian function'

$$f(p) = -M p_c \sqrt{\left( \frac{p+c}{p_c+c} - \left( \frac{p+c}{p_c+c} \right)^m \right) \left[ 2(1-\alpha) \frac{p+c}{p_c+c} + \alpha \right]}, \quad (15)$$

if  $\frac{p+c}{p_c+c} \in [0, 1]$ ,

and  $f(p) = +\infty$ , if  $(p+c)/(p_c+c) \notin [0, 1]$ . The Lode-dependence of yielding is described by the 'deviatoric function' (proposed by [12] and independently by [4])

$$g(\theta) = \frac{1}{\cos[\beta \frac{\pi}{6} - \frac{1}{3} \arccos(\gamma \cos 3\theta)]}. \quad (16)$$

The seven, non-negative material parameters

$$M > 0, \quad p_c > 0, \quad c \geq 0, \quad 0 < \alpha < 2, \quad m > 1, \quad 0 \leq \beta \leq 2, \quad 0 \leq \gamma < 1$$

define the shape of the associated yield surface. In particular,  $M$  controls the pressure-sensitivity,  $p_c$  and  $c$  are the yield strengths under ideal isotropic compression and tension, respectively. Parameters  $\alpha$  and  $m$  define the distortion of the meridian section, while  $\beta$  and  $\gamma$  model the shape of the deviatoric section.

### 2.3. An infinite class of hardening laws

In order to simulate the nonlinear hardening of concrete, the following class of hardening rules in incremental form is proposed:

$$\dot{p}_c = \frac{k_1}{(1 + \delta \pi_a)^n} \dot{\pi}_a, \quad (17)$$

$$\dot{c} = \Omega \dot{p}_c, \quad (18)$$

where four material parameters have been introduced:  $k_1 > 0$ ,  $\delta \geq 0$ ,  $n > 0$ , and  $0 < \Omega < 1$ .

A substitution of the flow rule (4) into (17) and (18) yields

$$\dot{p}_c = \dot{\lambda} \frac{k_1}{(1 + \delta \pi_a)^n} |\mathbf{P}|, \quad (19)$$

$$\dot{c} = \dot{\lambda} \frac{\Omega k_1}{(1 + \delta \pi_a)^n} |\mathbf{P}|. \quad (20)$$

Eqs. (17) and (18) can be integrated in order to obtain the hardening laws in finite form as follows

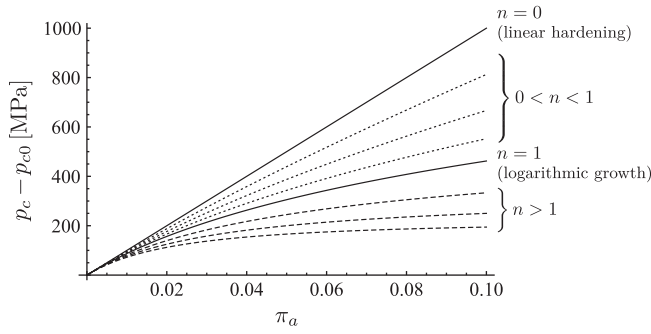


**Fig. 1.** The infinite class of hardening laws corresponding to Eq. (21). Curves are obtained by setting the parameters  $k_1$  and  $\delta$  to the conventional values  $k_1 = 10,000$  MPa,  $\delta = 30$ , and varying the parameter  $n$ .

$$p_c = \begin{cases} p_{c0} + \frac{k_1}{\delta} \log(1 + \delta \pi_a), & n = 1, \\ p_{c0} + \frac{k_1}{\delta} \frac{(1 + \delta \pi_a)^{n-1} - 1}{(n-1)(1 + \delta \pi_a)^{n-1}}, & n \neq 1, \end{cases} \quad (21)$$

$$c - c_0 = \Omega(p_c - p_{c0}). \quad (22)$$

In order to gain insight on the physical meaning of the proposed class of hardening rules, let us consider the asymptotic behaviour of the finite form (21) as  $\pi_a \rightarrow 0$ , which turns out to be independent of the parameters  $\delta$  and  $n$  and is given by the formula

$$p_c = p_{c0} + k_1 \pi_a + O(\pi_a^2). \quad (23)$$

This formula shows that, at an early stage of plastic deformation, the hardening is linear with a slope governed by the parameter  $k_1$ .

On the other hand, the hardening at a later stage of plastic deformation is governed by the parameters  $\delta$  and  $n$ . This is made clear by considering the asymptotic behaviour of the finite form (21) as  $\pi_a \rightarrow \infty$ :

$$p_c = \begin{cases} \frac{k_1}{\delta} \log(\delta \pi_a) + p_{c0} + \frac{k_1}{\delta^2 \pi_a} + O(\pi_a^{-2}), & n = 1, \\ p_{c0} + \frac{k_1}{(n-1)\delta} - \frac{k_1}{(n-1)\delta(\delta \pi_a)^{n-1}} + O(\pi_a^{-n}), & n \neq 1. \end{cases} \quad (24)$$

Note that, for  $0 < n \leq 1$ ,  $p_c$  turns out to be unbounded and for  $n = 1$  there is a logarithmic growth of hardening. For  $n > 1$ ,  $p_c$  is bounded (Fig. 1) with a limit value given by

$$p_{c0} + \frac{k_1}{(n-1)\delta}.$$

With the definition of the hardening law, the proposed elastoplastic constitutive model is ready to be calibrated, implemented and tested, which is the subject of the following Sections, where two members of the class of hardening laws will be analyzed, namely,  $n = 1$  and  $n = 2$ , the former corresponding to the logarithmic growth of hardening and the latter approaching the perfectly plastic behaviour.

### 3. Calibration of material parameters and comparison with experimental results

#### 3.1. Calibration of the BP yield surface

The BP yield surface has been calibrated on the basis of available experiments [6,7,9,10,14], to model the behaviour of concrete in the  $p$ - $q$  plane (Fig. 2) and in the biaxial  $\sigma_1/f_c$ - $\sigma_2/f_c$  plane (Fig. 3), where  $f_c$  (taken positive) defines the failure for compressive uniaxial stress. We have assumed a ratio between  $f_c$  and the failure stress in uniaxial tension  $f_t$  equal to 10. The parameter values which have been found to provide the better interpolation of

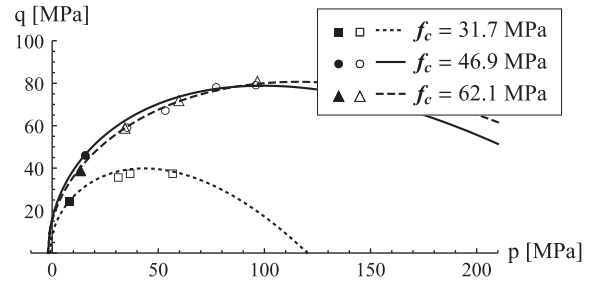


**Fig. 2.** The meridian section ( $p$ - $q$  plane) of the BP yield surface interpolating experimental results for three concretes (data taken from [7]). Black (white) spots denote results relative to unconfined (confined) compression.

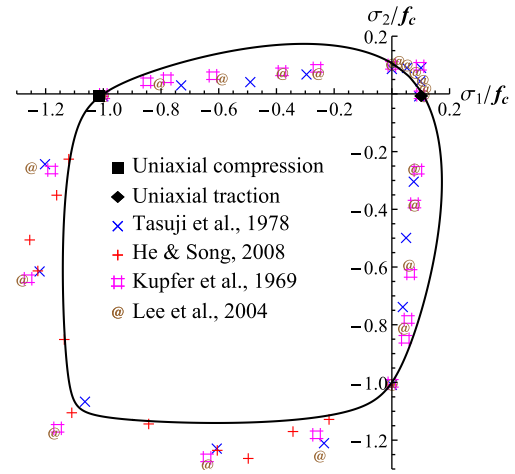


**Fig. 3.** The BP yield surface in the biaxial plane interpolating experimental results for concrete.

**Table 1**

Yield function parameters employed for the simulation of triaxial compression tests.

Concrete's compression strength	$M$	$m$	$\alpha$	$\beta$	$\gamma$	$p_c$ (MPa)	$c$ (MPa)
$f_c = 31.7$ MPa	0.435	2.5	1.99	0.6	0.98	120	1.02
$f_c = 46.9$ MPa	0.38	2	1.99	0.6	0.98	300	1.9
$f_c = 62.1$ MPa	0.33	2.5	1.99	0.6	0.98	320	2.1

experimental data for the three concretes (identified by their uniaxial compressive strengths  $f_c = 31.7$  MPa,  $f_c = 46.9$  MPa, and  $f_c = 62.1$  MPa) reported by [7] are given in Table 1.

#### 3.2. A validation of the model against triaxial tests

The above-presented constitutive model has been implemented in a UMAT routine of ABAQUS Standard Ver. 6.11 [1].

Triaxial compression tests at high pressure on cylindrical concrete specimen (experimental data taken from [7]) have been simulated using two different hardening laws of the class (17)–(18), namely  $n = 1$ , corresponding to logarithmic hardening, and  $n = 2$ , which provides a smooth transition to perfect plasticity. The values of parameters (identifying elastic behaviour and hardening) used in the simulations are reported in Table 2.

Results of the numerical simulations (one axisymmetric biquadratic finite element with eight nodes – so called ‘CAX8’ – has been employed) are presented in Figs. 4–6, reporting the axial stress  $\sigma_{11}$  plotted in terms of axial  $\epsilon_{11}$  and radial  $\epsilon_{22}$  strains. The three figures

**Table 2**

Elastic and hardening parameters employed for the simulation of triaxial compression tests.

Material	$E$ (MPa)	$\nu$	$k_1$ (MPa)	$\delta$	$\Omega$
$f_c = 31.7$ MPa					
$n = 1$	13,000	0.18	25,000	220	0.0085
$n = 2$	13,000	0.18	25,000	80	0.0085
$f_c = 46.9$ MPa					
$n = 1$	11,200	0.18	223,000	2300	0.00633
$n = 2$	11,200	0.18	100,000	190	0.00633
$f_c = 62.1$ MPa					
$n = 1$	43,000	0.18	210,000	220	0.00656
$n = 2$	43,000	0.18	210,000	220	0.00656

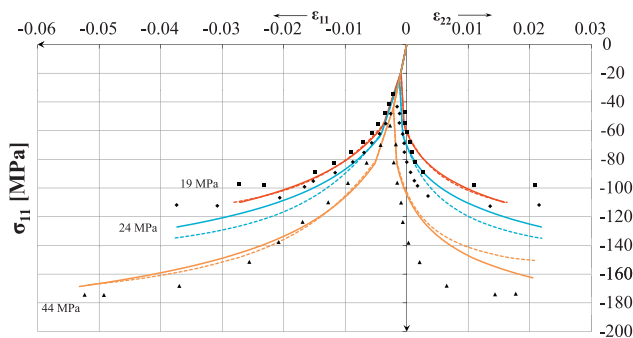


**Fig. 4.** Comparison between the simulation of triaxial tests at different confining pressures and the relative experiments (taken from [7], concrete with  $f_c = 31.7$  MPa). The solid [the dashed] lines correspond to the case  $n = 1$  [ $n = 2$ ].

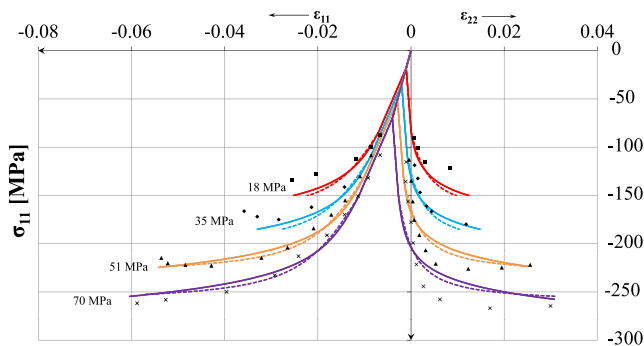


**Fig. 5.** Comparison between the simulation of triaxial tests at different confining pressures and the relative experiments (taken from [7], concrete with  $f_c = 46.9$  MPa). The solid [the dashed] lines correspond to the case  $n = 1$  [ $n = 2$ ].

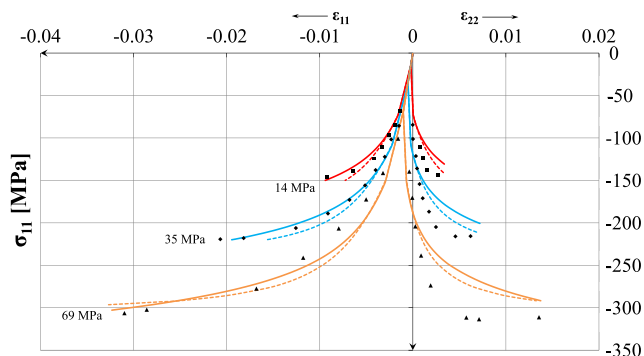


**Fig. 6.** Comparison between the simulation of triaxial tests at different confining pressures and the relative experiments (taken from [7], concrete with  $f_c = 62.1$  MPa). The solid [the dashed] lines correspond to the case  $n = 1$  [ $n = 2$ ].

refer to the three different concretes, identified by their different uniaxial compressive strength. Different colours<sup>2</sup> of the lines denote simulations performed at different confining pressure, namely: {19, 24, 44} MPa for Fig. 4, {18, 35, 51, 70} MPa for Fig. 5, and {14, 35, 69} MPa for Fig. 6.

The solid lines correspond to the logarithmic hardening laws (21) and (22) with  $n = 1$ . The dashed lines correspond to the hardening laws (21) and (22) with  $n = 2$ .

It is clear from the figures that both the hardening laws perform correctly, but the hardening rule with  $n = 1$  leads to a more stable numerical behaviour, while with  $n = 2$  failure can be approached.

## 4. Conclusions

A reasonably simple inelastic model for concrete has been formulated on the basis of a recently-proposed yield function and a class of hardening rules, which may describe a smooth transition from linear elastic to perfectly plastic behaviour. The model has been implemented into a numerical routine and successfully validated against available triaxial experiments at different confining pressures. Although the presented constitutive approach cannot compete in accuracy with more sophisticated models, it has been proven to be robust for numerical calculations, so that it results particularly suitable for complex design situations where easy of calibration, fast convergence and stability become important factors.

## Acknowledgments

Part of this work was prepared during secondment of D.B. at Enginsoft (TN). D.B. and A.P. gratefully acknowledge financial support from European Union FP7 project under contract number PIAP-GA-2011-286110-INTERCER2. S.R.B. gratefully acknowledges financial support from European Union FP7 project under contract number PIAP-GA-2013-609758-HOTBRICKS.

## References

- [1] Abaqus 6.11, 2011. User Manual <<http://simulia.com>>.
- [2] Bazant ZP, Adley MD, Carol I, Jirasek M, Akers SA, Rohani B, Cargile JD, Caner FC. Large-strain generalization of microplane model for concrete and application. *J. Eng. Mech.-ASCE* 2000;126:971–80.
- [3] Bigoni D. Nonlinear Solid Mechanics. Bifurcation Theory and Material Instability. Cambridge University Press; 2012.
- [4] Bigoni D, Piccolroaz A. Yield criteria for quasibrittle and frictional materials. *Int. J. Solids Struct.* 2004;41:2855–78.
- [5] Chen WF, Han DJ. Plasticity for structural engineers. Springer-Verlag; 1988.
- [6] He Z, Song Y. Failure mode and constitutive model of plain high-strength high-performance concrete under biaxial compression after exposure to high temperatures. *Acta Mech. Solida Sinica* 2008;21:149–59.
- [7] Kotsovos MD, Newman JB. Mathematical description of deformational behavior of concrete under generalized stress beyond ultimate strength. *ACI J* 1980;77:340–6.
- [8] Krajcinovic D, Basista M, Sumarac D. Micromechanically inspired phenomenological damage model. *J. Appl. Mech. ASME* 1991;58:305–10.
- [9] Kupfer, H., Hilsdorf, H.K., Rusch, H. (1969) Behaviour of concrete under biaxial stress. *Proc. ACI* 66, 656–666.
- [10] Lee S-K, Song Y-C, Han S-H. Biaxial behavior of plain concrete of nuclear containment building. *Nucl. Eng. Des.* 2004;227:143–53.
- [11] Piccolroaz A, Bigoni D. Yield criteria for quasibrittle and frictional materials: a generalization to surfaces with corners. *Int. J. Solids Struct.* 2009;46:3587–96.
- [12] Podgórski J. General failure criterion for isotropic media. *J. Eng. Mech. ASCE* 1985;111:188–99.
- [13] Schaufert EA, Cusatis G. Lattice Discrete Particle Model for Fiber-Reinforced Concrete. I: Theory. *J. Eng. Mech. ASCE* 2012;138:826–33.
- [14] Tasuji ME, Slate FO, Nilson AH. Stress-strain response and fracture of concrete in biaxial loading. *ACI J* 1978;75:306–12.
- [15] Yazdani S, Schreyer HL. Combined plasticity and damage mechanics model for plain concrete. *J. Eng. Mech.-ASCE* 1990;116:1435–50.

<sup>2</sup> For interpretation of colour in Figs. 4–6, the reader is referred to the web version of this article.